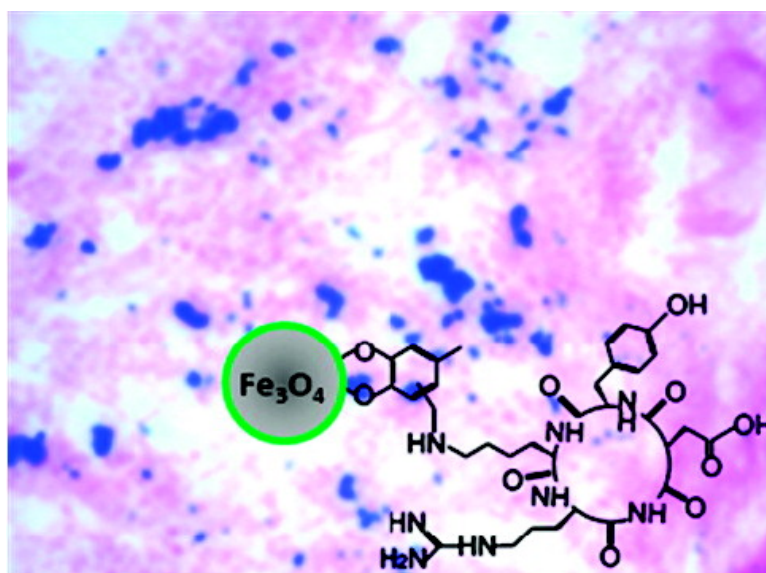


Ultrasmall c(RGDyK)-Coated FeO Nanoparticles and Their Specific Targeting to Integrin $\alpha_5\beta_1$ -Rich Tumor Cells

Jin Xie, Kai Chen, Ha-Young Lee, Chenjie Xu, Andrew R. Hsu, Sheng Peng, Xiaoyuan Chen, and Shouheng Sun

J. Am. Chem. Soc., **2008**, 130 (24), 7542-7543 • DOI: 10.1021/ja802003h • Publication Date (Web): 24 May 2008

Downloaded from <http://pubs.acs.org> on February 8, 2009



More About This Article

Additional resources and features associated with this article are available within the HTML version:

- Supporting Information
- Links to the 4 articles that cite this article, as of the time of this article download
- Access to high resolution figures
- Links to articles and content related to this article
- Copyright permission to reproduce figures and/or text from this article

[View the Full Text HTML](#)

Ultrasmall c(RGDyK)-Coated Fe₃O₄ Nanoparticles and Their Specific Targeting to Integrin $\alpha_v\beta_3$ -Rich Tumor Cells

Jin Xie,[†] Kai Chen,[‡] Ha-Young Lee,[‡] Chenjie Xu,[†] Andrew R. Hsu,[‡] Sheng Peng,[†] Xiaoyuan Chen,^{*,‡} and Shouheng Sun^{*,†}

Department of Chemistry, Brown University, Providence, Rhode Island 02912, and Molecular Imaging Program at Stanford (MIPS), Bio-X, and Biophysics, Department of Radiology, Stanford University, 1201 Welch Road P095, Stanford, California 94305-5484

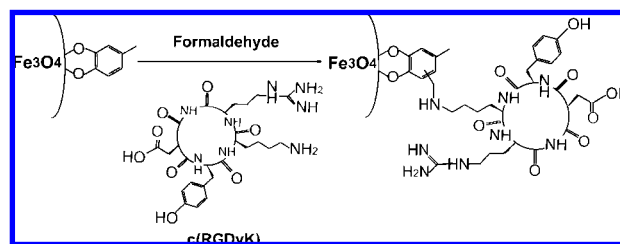
Received March 18, 2008; E-mail: ssun@brown.edu; shawchen@stanford.edu

Noninvasive detection of tumors at an early stage by magnetic resonance imaging (MRI) needs highly sensitive contrast agents. Synthesized from solution phase and coated with various hydrophilic molecules, iron oxide nanoparticles (IONPs) can be well stabilized in biological systems and used for T₂ contrast enhancement in MRI.^{1–3} However, commonly used IONP contrast agents require nonspecific uptake by mononuclear phagocytes to improve the local contrast, and at the hydrodynamic size of over 50 nm, these particles have very limited extravasation ability and are subject to easy uptake by the reticuloendothelial system (RES),^{4,5} which undermines severely their targeting specificity. To overcome the problems of nonspecific uptake and to enhance the extra-vascular ability, even smaller hydrodynamic sizes are desired.^{5,6} Despite recent synthetic progresses, making small (<10 nm hydrodynamic size) IONPs with required biocompatibility and targeting capability is still extremely challenging.

Here, we present a direct synthesis of ultrasmall Fe₃O₄ NPs (<10 nm in hydrodynamic diameter) and demonstrate their *in vivo* tumor-specific targeting capability. The Fe₃O₄ NPs with 4.5 nm core size were synthesized by thermal decomposition of iron pentacarbonyl, Fe(CO)₅, followed by air oxidation. Different from any of the previous synthesis methods,⁷ the current preparation used a new ligand 4-methylcatechol (4-MC) as the surfactant. More importantly, the 4-MC coated IONP surface was directly conjugated with a peptide, c(RGDyK), via the Mannich reaction, rendering the particles stable in physiological environment. The synthesis is illustrated in Scheme 1. The c(RGDyK)-MC-Fe₃O₄ NPs have an overall diameter of ~8.4 nm and are stable in physiological conditions. They can target specifically to integrin $\alpha_v\beta_3$ -rich tumor cells. When administrated intravenously, these c(RGDyK)-MC-Fe₃O₄ NPs accumulate preferentially in tumor cells, which are readily tracked by MRI.

Fe₃O₄ NPs were synthesized by thermal decomposition of Fe(CO)₅ in benzyl ether in the presence of 4-MC followed by air oxidation.⁸ Because of the formation of a strong chelate bond between iron and a catechol unit,⁹ 4-MC forms a tight thin coating layer around the NP surface. The sizes of the NPs (from 2.5–5 nm as shown in Figure S1) were tunable by the MC/Fe ratio. Figure 1A shows the high resolution transmission electron microscopy (HRTEM) image of the 4.5 nm Fe₃O₄ NPs. The inverse spinel structure of the Fe₃O₄ NPs was characterized by X-ray diffraction (XRD) analysis (Figure S2). The 4-MC coating was confirmed by FTIR (Figure 1B), from which three aromatic C=C stretch peaks at 1602, 1521, and 1415 cm⁻¹ are attributed to the coated 4-MC and are right-shifted compared to those from the free 4-MC (1623, 1527, and 1448 cm⁻¹). Peaks at 624, 594,

Scheme 1. Schematic Illustration of Coupling c(RGDyK) Peptide to Fe₃O₄ NPs



and 445 cm⁻¹ are typical Fe–O absorption bands.¹⁰ The MC-Fe₃O₄ NPs were well dispersed in chloroform (CHCl₃) or dimethylformamide (DMF), ready for further functionalization.

The aromatic ring of 4-MC around the Fe₃O₄ NPs can be directly coupled with amine (NH₂) group via a Mannich reaction, offering a direct method for Fe₃O₄ functionalization. Here we choose to conjugate a cyclic RGD peptide, c(RGDyK), to the NP surface. This head-to-tail cyclized RGD peptide has been proven to target specifically to the activated endothelial cells and various tumor cells expressing cell adhesion molecule integrin $\alpha_v\beta_3$.¹¹ The coupling via a Mannich reaction was performed by mixing the MC-Fe₃O₄ NPs with c(RGDyK) and formaldehyde (HCHO) in DMF (Scheme 1).⁸

The RGD coated Fe₃O₄ NPs are stable for months without precipitation in aqueous dispersion (Figure S3). The overall size of the particles, measured by dynamic light scattering (DLS) in water, is 8.4 ± 1.0 nm (Supporting Information, Figure S3), close to the simple addition of the ~4.5 nm core (Figure 1A) and ~2 nm coating of 4-MC + c(RGDyK). The matrix-assisted laser desorption ionization-mass spectrometry (MALDI-MS) shows various M/Z peaks (Figure S4) that confirm the successful conjugation of c(RGDyK) to 4-MC. The number of RGD peptide per particle was estimated to be 100–200.⁸

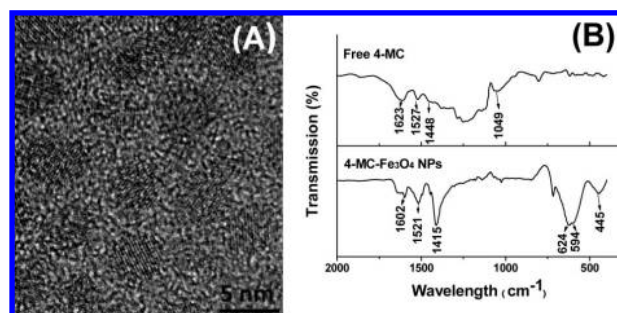


Figure 1. (A) HRTEM image of the as-synthesized, 4.5 nm MC-Fe₃O₄ NPs; (B) FTIR spectra of the free 4-MC and MC-Fe₃O₄ NPs.

[†] Brown University.

[‡] Stanford University.

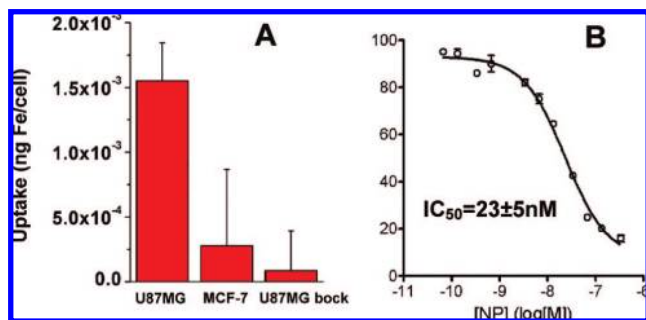


Figure 2. (A) Cell uptake of c(RGDyK)-MC-Fe₃O₄ NPs by U87MG, MCF-7, and U87MG + c(RGDyK) block, and (B) the c(RGDyK)-MC-Fe₃O₄ NP concentration dependent replacement of ¹²⁵I-echistatin on U87MG cells.

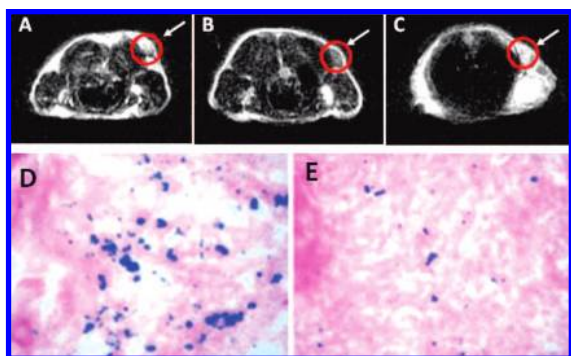


Figure 3. MRI of the cross section of the U87MG tumors implanted in mice: (A) without NPs, (B) with the injection of 300 μg of c(RGDyK)-MC-Fe₃O₄ NPs, and (C) with the injection of c(RGDyK)-MC-Fe₃O₄ NPs and blocking dose of c(RGDyK); and Prussian blue staining of U87MG tumors in the presence of (D) c(RGDyK)-MC-Fe₃O₄ NPs and (E) c(RGDyK)-MC-Fe₃O₄ NPs plus blocking dose of c(RGDyK).

To study integrin targeting specificity of the c(RGDyK)-MC-Fe₃O₄ NPs, we incubated these NPs with both U87MG human glioblastoma (high $\alpha_v\beta_3$) and MCF-7 human breast cancer (low $\alpha_v\beta_3$) cell lines at 37 °C for 30 min. The iron concentration within the cells were analyzed by inductively coupled plasma atomic emission spectroscopy (ICP-AES).⁸ Figure 2A shows the Fe uptake for U87MG cells, which is about 5-fold higher than that of MCF-7 cells. The accumulation of NPs in U87MG cells is effectively inhibited in the presence of the blocking dose (2 μM) of c(RGDyK), further demonstrating integrin specificity of c(RGDyK)-MC-Fe₃O₄ NPs. The c(RGDyK)-MC-Fe₃O₄ NPs also show good binding ability to integrin. This is confirmed by the displacement competitive binding assay using $\alpha_v\beta_3$ positive U87MG cells, as shown in Figure 2B. The c(RGDyK)-MC-Fe₃O₄ NPs inhibit ¹²⁵I-echistatin binding to integrin in a concentration dependent manner. The IC₅₀ value, used to measure the affinity of the binding agents, is calculated to be 23 ± 5 nM for NPs, which is significantly higher than monomeric RGD peptide (250 ± 60 nM). The enhanced binding affinity is from the multivalent effect as discussed previously.^{3,12}

The targeting ability of the c(RGDyK)-MC-Fe₃O₄ NPs to integrin $\alpha_v\beta_3$ in vivo was evaluated by T₂-weighted fast spin-echo MR imaging with mice bearing U87MG tumors. The r_2 relaxivity of the c(RGDyK)-MC-Fe₃O₄ NPs was measured to be 165 mM⁻¹s⁻¹ (Figure S5), which is larger than that of the commercial Feridex NPs (104 mM⁻¹s⁻¹) with similar core size.¹³ This larger r_2 value is likely caused by the stronger field perturbation around the NPs due to the thin c(RGDyK) coating. The tumor MR signal intensity decreased significantly (42 ± 5%) after injection of c(RGDyK)-MC-Fe₃O₄ NPs (Figure 3A,B). Such signal reduction was inhibited (15 ± 3%) in the presence

of a blocking dose of c(RGDyK) peptide (10 mg/kg) (Figure 3C), proving the specificity of the particle targeting in vivo. To further investigate the particle distribution in various organs, the animals were sacrificed immediately after the MR scan at 4 h time point, and Prussian blue staining was employed to visualize the disposition of the c(RGDyK)-MC-Fe₃O₄ NPs without and with the blocking dose of c(RGDyK) peptide (Figure 3D,E). Prominent blue spots on the U87MG tumor slices were observed (Figure 3D) and the blue spots were reduced in the presence of free c(RGDyK) (Figure 3E), further confirming that the accumulation of c(RGDyK)-MC-Fe₃O₄ NPs was mediated by integrin $\alpha_v\beta_3$ binding. Additionally, the c(RGDyK)-MC-Fe₃O₄ NPs were rarely seen in kidneys and muscle, indicating that the NPs sustained enough circulation time for targeting, even though some deposition in both liver and spleen were seen (Figure S6). The NPs in the tumor were mostly localized on the integrin expressing tumor vasculature and tumor cells with little to no macrophage uptake (Figure S7).

This report introduces a novel way of synthesizing and functionalizing ultrasmall Fe₃O₄ NPs as contrast agents for potential in vivo tumor detection using MRI. The Fe₃O₄ NPs are synthesized by thermal decomposition of Fe(CO)₅ in the presence of 4-MC followed by air oxidation. Mannich reaction is applied to couple NH₂-terminated peptide c(RGDyK), and the c(RGDyK)-MC-Fe₃O₄ NPs show the desired biocompatibility and specificity to U87MG tumor cells. Compared to the free RGD peptide, the c(RGDyK)-MC-Fe₃O₄ NPs with desired size could dramatically increase the cellular uptake due to the multivalent binding. This new NP functionalization strategy can be readily extended to couple other bioactive molecules with amine functional group to Fe₃O₄ NPs. Further work on extravasation ability of the biofunctionalized IONPs for target-specific delivery is underway.

Acknowledgment. The work was supported by NIH/NCI 1R21CA12859-01 (S.S.), U54CA119367/R21CA121842 (X.C.) and in part by DOE/EPSCoR DE-FG02-07ER36374 (S.S.).

Supporting Information Available: Fe₃O₄ NP synthesis, surface functionalization and characterization. This material is available free of charge via the Internet at <http://pubs.acs.org>.

References

- (1) (a) Pankhurst, Q. A.; Connolly, J.; Jones, S. K.; Dobson, J. J. *Phys. D: Appl. Phys.* **2003**, *36*, R167–R181. (b) Lee, J. H.; Huh, Y. M.; Jun, Y.; Seo, J.; Jang, J.; Song, H. T.; Kim, S.; Cho, E. J.; Yoon, H. G.; Suh, J. S.; Cheon, J. *Nat. Med.* **2007**, *13*, 95–99.
- (2) Jun, Y. W.; Huh, Y. M.; Choi, J. S.; Lee, J. H.; Song, H. T.; Kim, S.; Yoon, S.; Kim, K. S.; Shin, J. S.; Suh, J. S.; Cheon, J. *J. Am. Chem. Soc.* **2005**, *127*, 5732–5733.
- (3) Montet, X.; Funovics, M.; Montet-Abou, K.; Weissleder, R.; Josephson, L. J. *Med. Chem.* **2006**, *49*, 6087–6093.
- (4) Moghimi, S. M.; Hunter, A. C.; Murray, J. C. *Pharm. Rev.* **2001**, *53*, 283–318.
- (5) Neuberger, T.; Schopf, B.; Hofmann, H.; Hofmann, M.; von Rechenberg, B. *J. Magn. Mag. Mater.* **2005**, *293*, 483–496.
- (6) Choi, H. S.; Liu, W.; Misra, P.; Tanaka, E.; Zimmer, J. P.; Ipe, B. I.; Bawendi, M. G.; Frangioni, J. V. *Nat. Biotechnol.* **2007**, *25*, 1165–1170.
- (7) (a) Park, J.; An, K. J.; Hwang, Y. S.; Park, J. G.; Noh, H. J.; Kim, J. Y.; Park, J. H.; Hwang, N. M.; Hyeon, T. *Nat. Mater.* **2004**, *3*, 891–895. (b) Sun, S. H.; Zeng, H.; Robinson, D. B.; Raoux, S.; Rice, P. M.; Wang, S. X.; Li, G. X. *J. Am. Chem. Soc.* **2004**, *126*, 273–279.
- (8) See Supporting Information.
- (9) Xu, C. J.; Xu, K. M.; Gu, H. W.; Zheng, R. K.; Liu, H.; Zhang, X. X.; Guo, Z. H.; Xu, B. *J. Am. Chem. Soc.* **2004**, *126*, 9938–9939.
- (10) Ma, M.; Zhang, Y.; Yu, W.; Shen, H. Y.; Zhang, H. Q.; Gu, N. *Colloids Surf. A: Physicochem. Eng. Asp.* **2003**, *212*, 219–226.
- (11) (a) Li, Z. B.; Cai, W. B.; Cao, Q. Z.; Chen, K.; Wu, Z. H.; He, L. N.; Chen, X. Y. *J. Nucl. Med.* **2007**, *48*, 1162–1171. (b) Cai, W. B.; Shin, D. W.; Chen, K.; Gheysens, O.; Cao, Q. Z.; Wang, S. X.; Gambhir, S. S.; Chen, X. Y. *Nano Lett.* **2006**, *6*, 669–676.
- (12) Jiang, W.; Kim, B. Y. S.; Rutka, J. T.; Chan, W. *Nat. Nanotechnol.* **2008**, *3*, 145–150.
- (13) Seo, W. S.; Lee, J. H.; Sun, X. M.; Suzuki, Y.; Mann, D.; Liu, Z.; Terashima, M.; Yang, P. C.; McConnell, M. V.; Nishimura, D. G.; Dai, H. *J. Nat. Mater.* **2006**, *5*, 971–976.

JA802003H